Organic Electronics 14 (2013) 1170–1176

Contents lists available at SciVerse ScienceDirect

Organic Electronics

journal homepage: www.elsevier.com/locate/orgel

Pentacene organic thin-film transistors with solution-based gelatin dielectric

Lung-Kai Mao [a], Jenn-Chang Hwang [a,*], Ting-Hao Chang [a], Chao-Ying Hsieh [a], Li-Shiuan Tsai [a], Yu-Lun Chueh [a], Shawn S.H. Hsu [b], Ping-Chiang Lyu [c], Ta-Jo Liu [d]

[a] Department of Materials Science and Engineering, National Tsing Hua University, Hsin-Chu City 30043, Taiwan
[b] Department of Electrical Engineering, National Tsing Hua University, Hsin-Chu City 30043, Taiwan
[c] Department of Life Science, National Tsing Hua University, Hsin-Chu City 30043, Taiwan
[d] Department of Chemical Engineering, National Tsing Hua University, Hsin-Chu City 30043, Taiwan

ARTICLE INFO

Article history:
Received 19 October 2012
Received in revised form 2 February 2013
Accepted 13 February 2013
Available online 26 February 2013

Keywords:
Gelatin
Field-effect mobility
OTFT
Pentacene

ABSTRACT

Gelatin is a natural protein in the field of food, pharmaceutical and tissue engineering, which works very well as the gate dielectric for pentacene organic thin-film transistors (OTFTs). An aqueous solution process has been applied to form a gelatin thin film on poly(ethylene terephthalate) (PET) or glass by spin-coating and subsequent casting. The device performance of pentacene OTFTs depend on the bloom number (molecular weight) of gelatin. The pentacene OTFT with 300 bloom gelatin as the gate dielectric in air ambient exhibits the best performance with an average field-effect mobility (μ_{FE}) value of ca. 16 $cm^2 V^{-1} s^{-1}$ in the saturation regime and a low threshold voltage of −1 V. The high performance of the pentacene OTFT in air ambient is attributed to the water resided in gelatin. The crystal quality of pentacene is not the key factor for the high performance.

1. Introduction

Organic thin-film transistors (OTFTs) are attractive for soft electronics because of flexibility, lightweight, large-area applicability and low cost [1,2]. One of the objectives in the research of OTFTs is to raise up the field-effect mobility (μ_{FE}) comparable to inorganic thin-film transistors (TFTs) so that OTFTs can be applied in practical applications such as e-paper, radio-frequency identification (RFID) tags, and biosensors [3–7].

The device performance of OTFTs strongly depends on the choice of gate dielectric, although carriers transports along the channel in the organic semiconducting layer during operation [8–10]. A simple approach to enhance μ_{FE} is to select properly a gate dielectric material in match with the chosen organic semiconductor in OTFTs. For instance, various gate dielectrics have been reported for pentacene OTFTs in the past, such as poly(methyl methacrylate) (PMMA), poly(vinyl pyrrolidone) (PVP), TiO_2-polymer composite, chicken albumen, silk fibroin and AlN [11–17]. Among them, silk fibroin have attracted attention since it may raise up the μ_{FE} value to ca. 23 $cm^2 V^{-1} s^{-1}$ reported by Wang et. al. [15]. The μ_{FE} value is higher than amorphous $InGaO_3(ZnO)_5$ (a-IGZO) TFTs [18].

Silk fibroin is a natural protein and surprisingly serves as an excellent gate dielectric for pentacene to deposit on. The enhanced crystal quality of pentacene on silk fibroin results in a very high μ_{FE} value. The success of silk fibroin in pentacene OTFTs supports that a complex protein structure may be in good match with small molecules such as pentacene at the molecular level. In order to understand deeper the role of natural protein in the device performance of OTFTs, we further investigate the possibility of using other natural proteins as the gate dielectric.

Gelatin is a low-cost natural protein with biocompatible, bioresorbable and biodegradable characteristics. It may be extracted from bone, skin, cartilage and connective tissues. Gelatin has been extensively applied in fields of food, pharmaceutical and tissue engineering. In drug

* Corresponding author. Tel.: +886 3 5722577.
E-mail address: jch@mx.nthu.edu.tw (J.-C. Hwang).

1566-1199/$ - see front matter © 2013 Elsevier B.V. All rights reserved.
http://dx.doi.org/10.1016/j.orgel.2013.02.010

delivery and tissue engineering applications, gelatin has been processed into various nano- or micro-spheres such as nano and microgels [19–22]. In this article, we present the device performance of OTFTs with type A gelatin as the gate dielectric. In general, gelatin contains major amino acids of glycine (Gly), proline (Pro), and 4-hydroxyproline (Hyp). The typical amino acid sequence of the type A gelatin has been reported to be Ala-Gly-Pro-Arg-Gly-Glu-4Hyp-Gly-Pro [23]. The gelatin thin film for OTFTs is formed by casting, which works very well as the gate dielectric for high performance pentacene OTFTs although its ammonic acids are quite different from silk fibroin.

2. Materials and methods

The type A gelatin (Sigma–Aldrich) of 70, 175 or 300 bloom was chosen to prepare the aqueous solution of gelatin (16% w/v) by dispersing 16 g gelatin powders in 100 ml distilled water and followed by heating on a hotplate with stirring at 80 °C for 30 min. The bottom gate configuration was used to fabricate pentacene OTFTs with gelatin as the gate dielectric, which is sketched in Fig. 1a. A gelatin thin film was coated onto a poly(ethylene terephthalate) (PET) or glass substrate patterned with 70 nm Au gate electrodes by spin-coating and subsequent casting at 60 °C for 36 h. The secondary structures of the cast gelatin thin film were analyzed using Fourier transform infrared ray-attenuated total reflection (FTIR-ATR). The cast gelatin thin film on the Au gate electrode was determined to be ca. 1140 nm thick using field emission scanning electron microscopy (FESEM; Fig. 1b). Pentacene (99%, Sigma–Aldrich) without purification was put in a crucible before evaporation. A pentacene layer of 65 nm thick was thermally evaporated at room temperature onto the cast gelatin thin film through a shadow metal mask at a base pressure of 1×10^{-6} torr. The deposition rate of pentacene was kept at 0.3 Å/s that was monitored by a quartz crystal oscillator. The morphology of the pentacene layer of 65 nm was measured using atomic force microscope (AFM; Fig. 1c). 70-nm-thick Au was finally thermally deposited onto pentacene to define source and drain electrodes. The channel length and width were 50 μm and 600 μm, respectively. The device characteristics of OTFTs were measured using Agilent 4155C. Capacitance versus frequency curves in the range of 1 K to 1 MHz were taken to determine the dielectric constant of gelatin using Agilent 4284 impedance analyzer. Quasi-static capacitance versus voltage curves were taken by sweeping voltage across a MIM structure using Agilent B1500. The sweeping rate of voltage in the quasi-static capacitance method is the same as that used for taking transfer characteristics of OTFTs. The quasi-static capacitance value was more accurate in the derivation of μ_{FE}.

3. Results and discussion

3.1. Effect of molecular weight of gelatin on device performance

Pentacene OTFTS were fabricated on PET using gelatin of three different kinds of molecular weight [20,000–25,000 Mw (70 bloom), 40,000–50,000 Mw (175 bloom) and 50,000–100,000 Mw (300 bloom)] as the gate dielectric. The μ_{FE} value in the saturation regime ($\mu_{FE,sat}$), the on/off current ratio, the threshold voltage, the subthreshold swing, and the maximum interface trap density (N_{SS}) value were derived from their output and transfer charac-

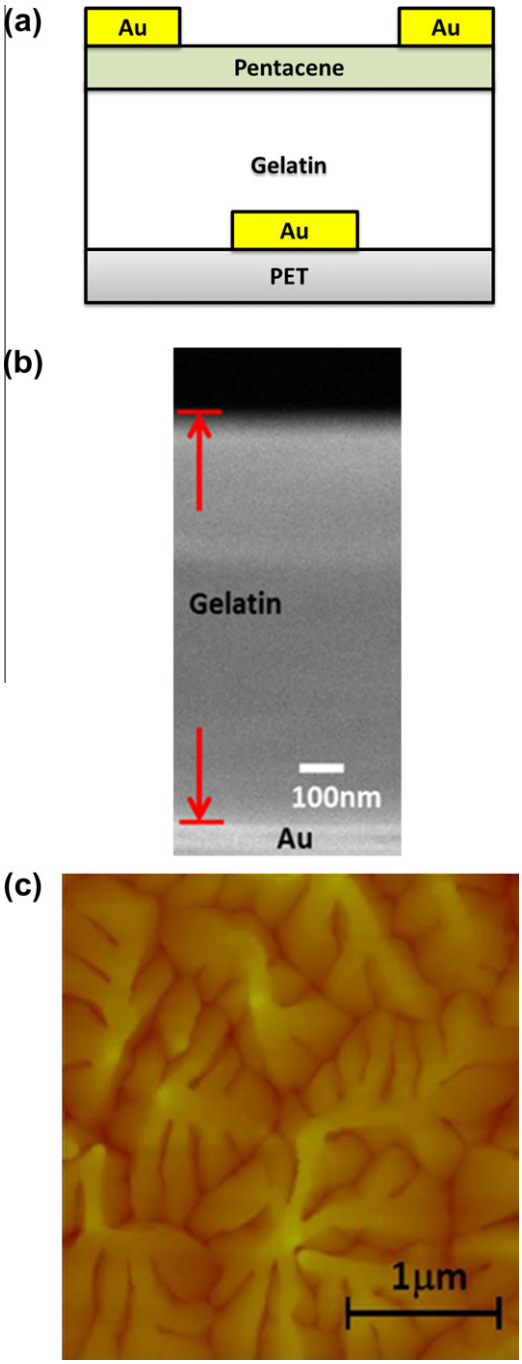

Fig. 1. (a) Schematic of the pentacene OTFT with gelatin as the gate dielectric. (b) Cross-sectional view of the FESEM image showing the thickness of the gelatin/Au/PET structure. The thickness of gelatin is ca. 1140 nm. (c) AFM image showing the morphology of the 65 nm pentacene layer on gelatin.

teristics taken in air ambient and summarized in Table 1. The average $\mu_{FE,sat}$ value increases from 8 $cm^2 V^{-1} s^{-1}$ to 16 $cm^2 V^{-1} s^{-1}$ when the molecular weight of gelatin increases from 70 to 300 bloom. We found that the surface energy of a gelatin thin film depends on the molecular weight, i.e. the bloom number. The water contact angle on the gelatin thin film was determined to be 75°, 78° and 84° for 70, 175 and 300 bloom number, respectively. The gelatin thin film with higher bloom number tends to be more hydrophobic. Better crystal quality of pentacene was reported easier to form on a hydrophobic surface [24,25]. This may explain that a higher $\mu_{FE,sat}$ value occurs for the case of 300 bloom gelatin since it exhibits a more hydrophobic surface.

Table 1
Device characteristics of pentacene OTFTs with gelatin of different molecular weight (i.e. bloom number).

Bloom number	70	175	300
Molecular weight (Da)	20–25 k	40–50 k	50–100 k
Concentration (wt%)	16	16	16
$\mu_{FE,sat}$ ($cm^2 V^{-1} s^{-1}$)	5–13	10–17	13–25
Average $\mu_{FE,sat}$ ($cm^2 V^{-1} s^{-1}$)	8	13	16
S.S. (mV/decade)	146	190	195
On/off ratio ($\times 10^3$)	7–10	5–10	0.5–1
Operation voltage (V)	−5	−5	−5
Leakage current (nA at −3 V)	4	6	2
N_{ss} ($\times 10^{11}$ cm^{-2} eV^{-1})	3.3–6	1.7–2.4	1.1–13
Average N_{ss} ($\times 10^{11}$ cm^{-2} eV^{-1})	4.4	2.3	6.1

The pentacene OTFT with 300 bloom gelatin exhibits optimum device performance, which is further characterized and presented as follows.

3.2. Properties of 300 bloom gelatin thin film

The gelatin thin film was formed by cross-linking the peptides of gelatin when the aqueous solution was cast at 60 °C for 36 h. The viscosity and surface tension of the

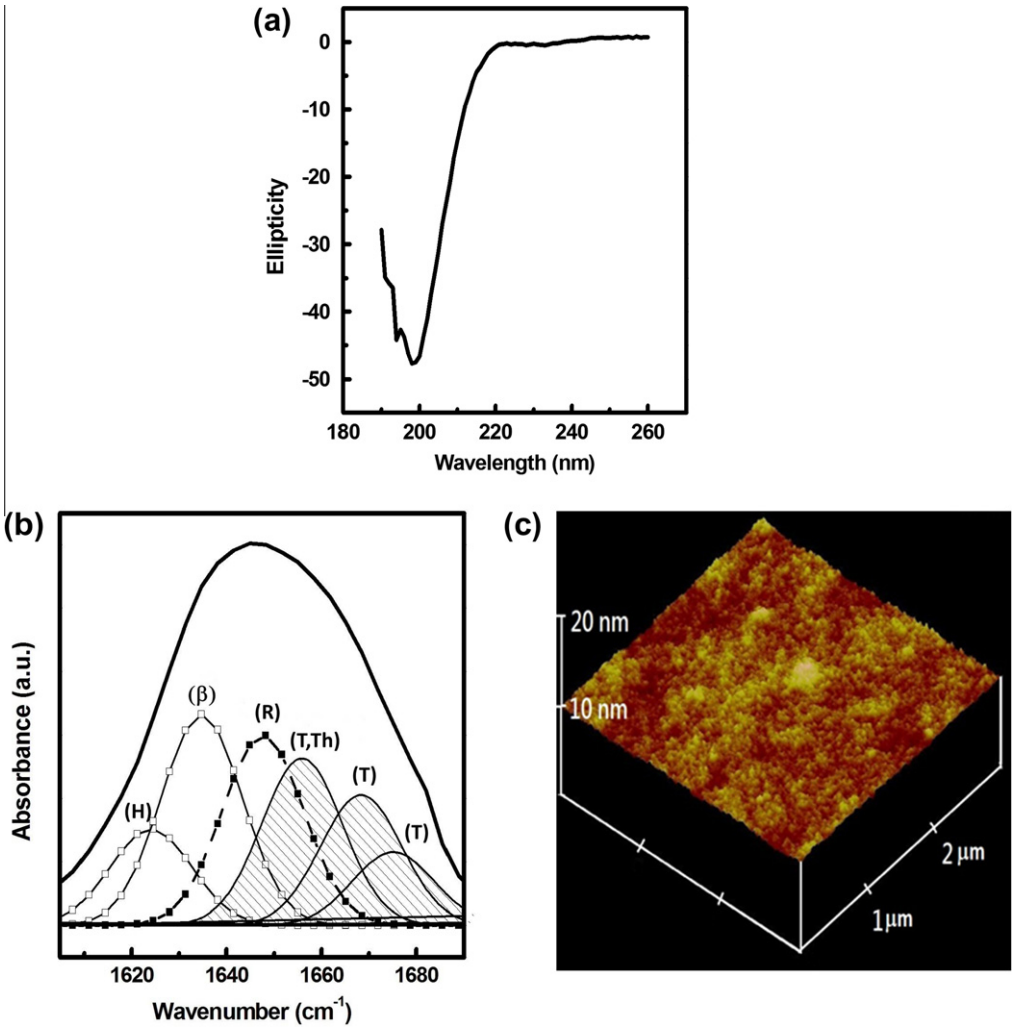

Fig. 2. Characterization of 300 bloom gelatin. (a) Circular dichroism spectrum. (b) FTIR-ATR spectrum showing the secondary structure. The gelatin consists of hydrogen-bonded (H), β-sheet (β), triple helix (Th), random coil (R), turn (T) according to the curve fitting results. (R: random coil; TH: triple helix; T: turn; β: β-sheet; H: hydrogen bonded C=O). (c) AFM images.

gelatin solution were measured to be 4.7 cp and 49 mN/m at 25 °C using viscosity (Brookfield DV-III+) and surface tension (Kyowa Interface Science CBVP-A3) analyzer, respectively. The secondary structure of gelatin in the solution was determined to be random-coil (Fig. 2a) using the circular dichroism spectroscopy (CD), consistent with the CD data reported by Cho and Song [26].

The secondary structures of gelatin in the cast thin film can be extracted from the FTIR-ATR spectrum around 1600–1700 cm^{-1} in Fig. 2b that is assigned to the peptide backbone of amide I. The amide I band represents the C═O stretching vibration of the amide group. The second derivative curve of the amide I spectrum is used to determine the number and positions of de-convoluted peaks. The gelatin thin film was determined to consist of H-bonds (H) at ca. 1624, β-sheet (β) at ca. 1634 cm^{-1}, random coil (R) at ca. 1647 cm^{-1}, triple helix (Th) at ca. 1656 cm^{-1}, β-turns (T) at ca. 1656, ca. 1668 and ca. 1675 cm^{-1}. The assignment of the vibration bands of amide I are based on previously published FTIR-ATR data [27–29].

To be a good gate dielectric for OTFTs, the gelatin thin film should meet some requirements such as low surface roughness, high dielectric constant (k) and low leakage current. First, the root-mean-square (RMS) roughness of the cast gelatin thin film surface was determined to be 0.37 nm using AFM (Fig. 2c). The RMS roughness value is similar to that of silk fibroin and flat enough to serve as the gate dielectric for pentacene OTFTs [15]. Second, the dielectric constant of gelatin was determined from 1 K to 1 MHz by using a metal–insulator–metal (MIM) structure. The capacitance value is ca. 5.8 nF/cm^2 at 1 MHz and slowly increases to ca. 7.1 nF/cm^2at 1 KHz, as shown in the capacitance versus frequency curve (Fig. 3a) taken in air ambient. The derived dielectric constant of gelatin increases from 7.5 at 1 MHz to 9.2 at 1 KHz as shown in the inset in Fig. 3a, which is much higher than the

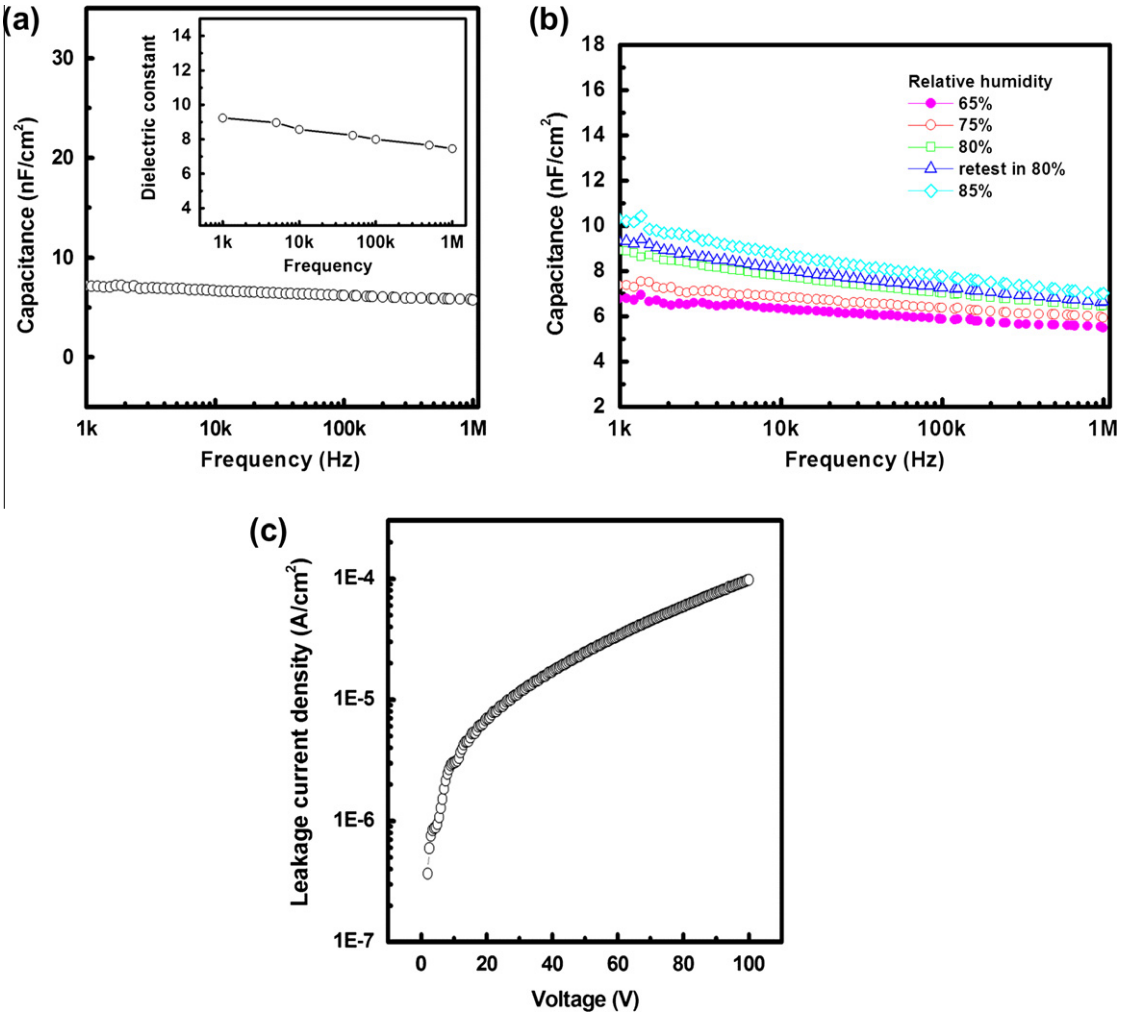

Fig. 3. Electrical characteristics of the MIM structure in air ambient with 300 bloom gelatin of ca. 1140 nm thick as the insulator. (a) Capacitance versus frequency curve from 1 K to 1 MHz on a log scale. Inset: Dielectric constant versus frequency curve. (b) Capacitance versus frequency curve in different humidity. (c) Leakage current density.

dielectric constant of SiO_2. Note that the capacitance value of gelatin increases slightly with relative humidity as shown in Fig. 3b. This is attributed to the absorption of water into the gelatin layer in the MIM structure in high humidity. The water inside the gelatin layer can be removed partially when relative humidity reduces from high to low. For instance, the capacitance does not completely reduce back to its value when the humidity is tuned from 85% to 80%, as shown in Fig. 3b.

The MIM structure was also used to determine the leakage current of the cast gelatin dielectric thin film. The leakage current density increases with voltage as shown in Fig. 3c. The leakage current density is lower than 1×10^{-4} A/cm^2 at voltage less than 100 V without breakdown. Therefore, the gelatin thin film may be used as a good dielectric.

3.3. Characteristics of pentacene OTFTs with 300 bloom gelatin as the gate dielectric

Fig. 4a shows the output characteristics of pentacene OTFT taken in air ambient of 65% humidity with good pinch-off and current saturation features. The humidity associated with the OTFT analysis condition is important since the gate capacitance value depends on humidity. The operation voltage in air ambient is less than 5 V. The $\mu_{FE,sat}$ value can be obtained from the transfer characteristics (Fig. 4b) using the equation:

$$I_{DS,sat} = (C_i \mu_{FE,sat} W/2L)(V_{GS} - V_{TH})^2 \quad (1)$$

where $I_{DS,sat}$, C_i, W, L, V_{GS} and V_{TH} denote the drain current density in the saturation regime, gate capacitance, channel width, channel length, gate voltage and threshold voltage, respectively. The inset is the $I_D^{1/2}$ versus V_G plot for the determination of $\mu_{FE,sat}$.

The capacitance value of 7.1 nF/cm^2 at 1 KHz is not appropriate for the determination of $\mu_{FE,sat}$ since the derived $\mu_{FE,sat}$ value is as high as 93.1 cm^2 V^{-1} s^{-1} [15]. To obtain an accurate $\mu_{FE,sat,}$ the C_i value was measured using the MIM structure next to the pentacene OTFT device at a sweep rate of 0.08 V/s in the quasi-state regime as shown in Fig. 4c. The quasi-static C_i value is estimated to be 26 nF/cm^2 using the maximum value. The accurate $\mu_{FE,sat}$

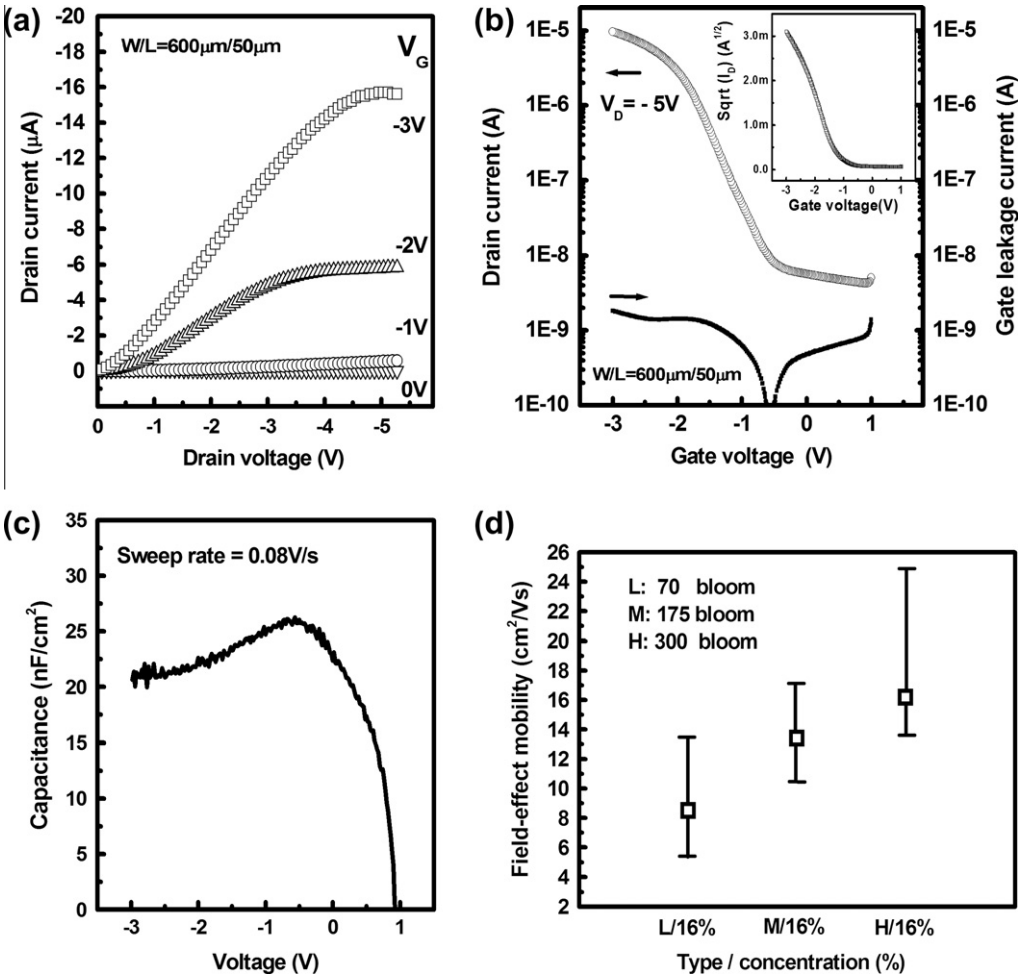

Fig. 4. Device characteristics of the pentacene OTFT and MIM in air ambient with 300 bloom gelatin as the dielectric insulator. (a) Output characteristics. (b) Transfer and gate leakage current characteristics. The inset is the $I_D^{1/2}$ versus V_G plot for the determination of $\mu_{FE,sat.}$ (c) Quasi-static capacitance versus voltage curve at a sweep rate of 0.08 V/s. (d) Mobility distribution of the pentacene OTFTs with gelatin of different molecular weight.

value is derived to be 25.5 $cm^2 V^{-1} s^{-1}$. The transfer characteristics in Fig. 4b show a low off-current of ca. 5.6×10^{-9} A, an on/off current ratio of 2×10^3, a low V_{TH} value of −1 V, and a subthreshold swing of 513 mV/decade.

The $\mu_{FE,sat}$ value increases with the molecular weight of gelatin as mentioned earlier in Table 1 and plotted in Fig. 4d. Note that the $\mu_{FE,sat}$ value scatters even for a certain molecular weight of gelatin. For instance, the $\mu_{FE,sat}$ value scatters from 13 to 25.5 $cm^2 V^{-1} s^{-1}$, collected from 25 OTFTs with 300 bloom gelatin as the gate dielectric. The average mobility is ca. 16 $cm^2 V^{-1} s^{-1}$.

3.4. Electrical characteristics of OTFTs under bending test in air ambient

The flexibility of the OTFTs was evaluated using a bending test under compressive mode. Fig. 5 shows the transfer characteristics of pentacene OTFT under 0.34% compressive strain taken in air ambient of 70% humidity. The compressive strain is estimated using the equation $\varepsilon = (d_f + d_s)/2R$ where d_f is the film thickness, d_s is the PET substrate thickness and R is the bending curvature radius [30,31]. The drain current slightly increases under 0.34% compressive strain. The derived $\mu_{FE,sat}$ and V_{TH} values are 14 $cm^2 V^{-1} s^{-1}$ and −0.6 V for the flatten sample. When the sample is under 0.34% compressive strain, $\mu_{FE,sat}$ reduces to 13.5 $cm^2 V^{-1} s^{-1}$ and V_{TH} decreases to −0.5 V.

3.5. Proposed mechanism

The high $\mu_{FE,sat}$ value of the OTFT taken in air ambient is attributed to the water resided in the gelatin thin film based on the following arguments. First, the output characteristics (Fig. 6a) taken in vacuum show good pinch-off and current saturation. The operation voltage in vacuum is much higher than that in air ambient. Moreover, the transfer characteristics (Fig. 6b) degrade when the OTFT is put in vacuum, compared with Fig. 4b. The drain current reaches ca. 1×10^{-5} A only at high gate voltage. The $\mu_{FE,sat}$ value in vacuum is derived to be 0.2 $cm^2 V^{-1} s^{-1}$, much less than that in air ambient. In contrast, the V_{TH} value is determined to be −15 V, much higher than −1 V taken in air ambient.

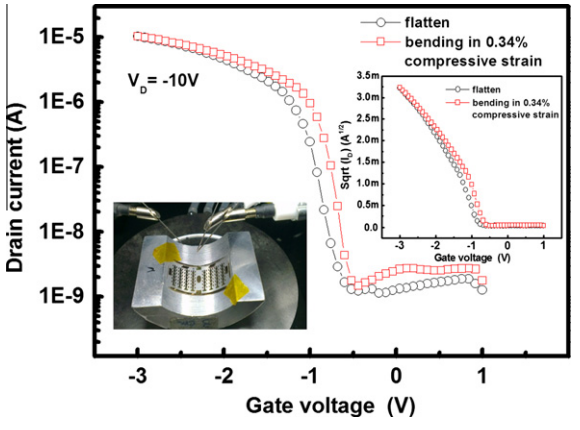

Fig. 5. Transfer characteristics of the pentacene OTFT under 0.34% compressive strain taken in air ambient of 70% humidity. The experimental set-up of the compressive bending test is inserted in the figure.

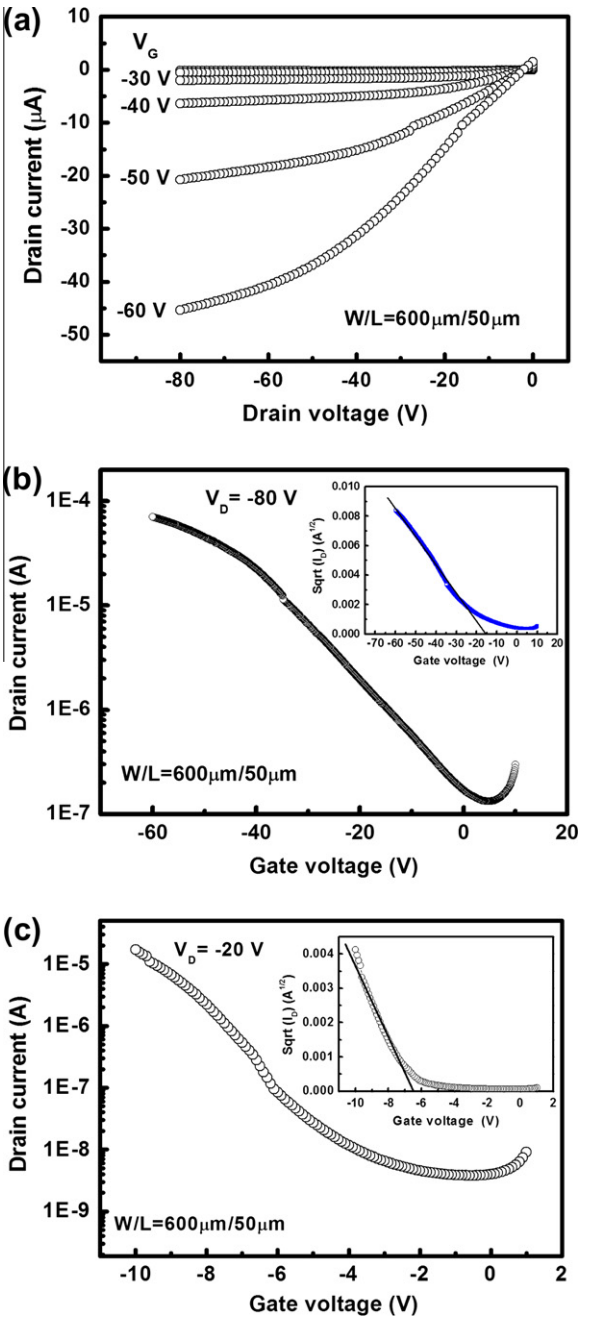

Fig. 6. Device characteristics of the pentacene OTFT with 300 bloom gelatin as the dielectric insulator. (a) Output characteristics in vacuum. (b) Transfer characteristics in vacuum. The inset is the $I_D^{1/2}$ versus V_G plot for the determination of $\mu_{FE,sat}$. (c) Transfer characteristics of the OTFT device exposed in air for 40 min. The inset is the $I_D^{1/2}$ versus V_G plot for the determination of $\mu_{FE,sat}$.

These data support that the constituents of air may affect the device performance in air ambient. And the crystal quality of pentacene itself is not the key factor for the high $\mu_{FE,sat}$ value in air ambient since the $\mu_{FE,sat}$ value in vacuum is low. Second, three constituents of air (nitrogen, oxygen and water) are considered able to diffuse into OTFTs and to enhance device performance in air ambient. The factors

of nitrogen and oxygen are excluded since the device performance remains about the same when the nitrogen or oxygen is purged into the vacuum chamber during taking I–V data. The enhancement of device performance in air ambient is then attributed to the water resides in gelatin, which is confirmed by exposing the OTFT device from vacuum back to air ambient. Fig. 6c shows the transfer characteristics of the OTFT device exposed from vacuum back to air for 40 min. The drain current increases and reaches ca. 10^{-5} A at $V_G = -10$ V. The $\mu_{FE,sat}$ value increases to 7 $cm^2 V^{-1} s^{-1}$ and the V_{TH} value reduces to -6.8 V after 40 min air exposure. The reduction of threshold voltage implies the existence of negatively charged ions inside the cast gelatin thin film. The negatively charged ions are proposed to be generated by the interaction of water with the polar OH-groups in ammonic acids in gelatin, similar to the work on PVP OTFTs [32,33]. The negative charged ions may help to attract more hole accumulation to fill the strap states before turn-on so that the V_{TH} value is lowered and the $\mu_{FE,sat}$ value is enhanced.

4. Conclusion

Our work illustrates that gelatin, a biomaterial, serves as a good gate dielectric for pentacene OTFTs. The OTFTs can operate at high speed (average $\mu_{FE,sat} = \sim 16$ $cm^2 V^{-1} s^{-1}$) and low voltage (5 V) in air ambient. The high device performance is attributed to negative charged ions generated by the interaction of water with the polar OH-group in ammonic acids in gelatin. The merits of gelatin for OTFTs are low cost, light-weight, flexibility, and solution process. A packaging method able to fix the amount of water resided in gelatin is important for this kind of OTFT devices in various applications, such as e-paper, RFID tags, and biosensors.

Acknowledgments

The authors like to thank Mr. Shih-Han Chen and Mr. Cheng-Lun Tsai for their technical assistance. The work is sponsored by National Science Council, Republic of China through the Project NSC 100-2221-E-007-067-MY3.

References

[1] G.H. Gelinck, H.E.A. Huitema, E. van Veenendaal, E. Cantatore, L. Schrijnemakers, J.B.P.H. van der Putten, T.C.T. Geuns, M. Beenhakkers, J.B. Giesbers, B.-H. Huisman, E.J. Meijer, E. Mena Benito, F.J. Touwslager, A.W. Marsman, B.J.E. van Rens, D.M. de Leeuw, Nat. Mater. 3 (2004) 106.
[2] J.A. Rogers, Z. Bao, K. Baldwin, A. Dodabalapur, B. Crone, V.R. Raju, V. Kuck, H. Katz, K. Amundson, J. Ewing, P. Drzaic, Proc. Natl. Acad. Sci. USA 98 (2001) 4835.
[3] C.D. Sheraw, L. Zhou, J.R. Huang, D.J. Gundlach, T.N. Jackson, Appl. Phys. Lett. 80 (2002) 1088.
[4] E. Cantatore, T.C.T. Geuns, G.H. Gelinck, E. van Veenendaal, A.F.A. Gruijthuijsen, L. Schrijnemakers, S. Drews, D.M. de Leeuw, IEEE J. Solid-State Circ. 42 (2007) 84.
[5] P.F. Baude, D.A. Ender, M.A. Haase, T.W. Kelley, D.V. Muyres, S.D. Theiss, Appl. Phys. Lett. 82 (2003) 3964.
[6] J.T. Mabeck, G.G. Malliaras, Anal. Bioanal. Chem. 84 (2006) 343.
[7] T. Someya, T. Sekitani, S. Iba, Y. Kato, H. Kawaguchi, T. Sakurai, Proc. Natl. Acad. Sci. USA 101 (2004) 9966.
[8] J. Veres, S. Ogier, G. Lloyd, Chem. Mater. 16 (2004) 4543.
[9] C. Bartic, H. Jansen, A. Campitelli, S. Borghs, Org. Electron. 3 (2002) 65.
[10] M.H. Yoon, H. Yan, A. Facchetti, T.J. Marks, J. Am. Chem. Soc. 127 (2005) 10388.
[11] T.G. Kim, E.H. Jeong, S.C. Lim, S.H. Kim, G.H. Kim, S.H. Kim, H.Y. Jeon, J.H. Youk, Synth. Met. 159 (2009) 749.
[12] H. Klauk, M. Halik, U. Zschieschang, G. Schmid, W. Radlik, J. Appl. Phys. 92 (2002) 5259.
[13] H.W. Zan, K.H. Yen, P.K. Liu, K.H. Ku, C.H. Chen, J.C. Hwang, Org. Electron. 8 (2007) 450.
[14] W.-C. Wang, C.-H. Wang, J.-Y. Lin, J.-C. Hwang, IEEE Trans. Electron Dev. 59 (2011) 1.
[15] C.-H. Wang, C.-Y. Hsieh, J.-C. Hwang, Adv. Mater. 23 (2011) 1630.
[16] J. Kim, S.H. Lim, Y.S. Kim, J. Am. Chem. Soc. 132 (2010) 42.
[17] J.-W. Chang, C.-G. Wang, C.-Y. Huang, T.-D. Tsai, T.-F. Guo, T.-C. Wen, Adv. Mater. 23 (2011) 4077.
[18] K. Nomura, H. Ohta, A. Takagi, T. Kamiya, M. Hirano, H. Hosono, Nature 432 (2004) 488.
[19] M.A. Vandelli, M. Romagnoli, A. Monti, M. Gozzi, P. Guerra, F. Rivasi, F. Forni, J. Control Release 96 (2004) 67.
[20] T. Coviello, P. Matricardi, C. Marianecci, F. Alhaique, J. Control Release 119 (2007) 5.
[21] J.K. Oh, D.I. Lee, J.M. Park, Prog. Polym. Sci. 34 (2009) 1261.
[22] A. Khademhosseini, R. Langer, Biomaterials 28 (2007) 5087.
[23] Thawatchai. Tungkavet, Datchanee. Pattavarakorn, Anuvat. Sirivat, J. Polym. Res. 19 (2012) 9759.
[24] Sang Yoon Yang, Kwonwoo Shin, Chan Eon Park, Adv. Funct. Mater. 15 (2005) 1806.
[25] D. Knipp, R.A. Street, A. Volkel, J. Ho, J. Appl. Phys. 93 (2003) 347.
[26] Y.S. Cho, K.B. Song, Biosci. Biotech. Biochem. 61 (1997) 1194.
[27] D.A. Prystupa, A.M. Donald, Polym. Gels Netw. 4 (1996) 87.
[28] A. Dong, P. Huang, W.S. Caughey, Biochemistry 29 (1990) 3303.
[29] J.H. Muyonga, C.G.B. Cole, K.G. Duodu, Food Chem. 86 (2004) 325.
[30] Chanwoo Yang, Jinhwan Yoon, Se Hyun Kim, Kipyo Hong, Dae Sung Chung, Kyuyoung Heo, Chan Eon Park, Moonhor Ree, Appl. Phys. Lett. 92 (2008) 243305.
[31] Fang-Chung Chen, Tzung-Da Chen, Bing-Ruei Zeng, Ya-Wei Chung, Semicond. Sci. Technol. 26 (2011) 034005.
[32] T. Jung, A. Dodabalapur, R. Wenz, S. Mohapatra, Appl. Phys. Lett. 87 (2005) 182109.
[33] S. Lee, B. Koo, J. Shin, E. Lee, H. Park, H. Kim, Appl. Phys. Lett. 88 (2006) 162109.